Comparison of IR-Transmission Method with the Conventional DTA Method (Kissinger Plot) in the Crystallization Study of Iron Tellurite Glass

Tetsuaki NISHIDA,* Satoru INOUE,† and Yoshimasa TAKASHIMA
Department of Chemistry, Faculty of Science, Kyushu University,
Hakozaki, Higashi-ku, Fukuoka 812
† National Institute for Research in Inorganic Materials, Science and Technology Agency,
Namiki 1-1, Tsukuba, Ibaraki 305
(Received March 19, 1992)

IR-transmission spectra of $95TeO_2 \cdot 5Fe_2O_3$ glass piece show a gradual decrease in the transmittance due to the crystallization initiating at the surface and spreading to the bulk. XRD, IR absorption spectra, and ^{57}Fe-Mössbauer spectra show the formation of paratellurite (α-TeO_2) and iron tellurite in the glass matrix. Johnson–Mehl–Avrami plot yields the activation energy (E_a) of 2.9±0.3 eV for the crystallization when the crystallized fraction is approximated by the decreased fraction of IR-transmittance. The E_a is identical to the Te–O single bond energy (3.0 eV) obtained from the literature. Kissinger plot of DTA used for the crystallization in the bulk yields E_a of 2.3 eV. These results indicate that the crystallization proceeds in a two- or three-dimensional manner by the diffusion process both in the bulk and at the surface. Ar^+-laser irradiation of $95TeO_2 \cdot 5Fe_2O_3$ glass results in a decrease in the IR-transmittance, indicating the "optical memory" effect.

Tellurite glasses have optical non-linearity and high transparency in the visible-to-IR region. Relatively low glass transition temperature (T_g) is of advantage for the preparation of so-called advanced materials, e.g., an "optical memory" device that will be utilized in the field of optoelectronics. It is important to elucidate the relationship between the crystallization and optical properties and also the mechanism of crystallization, since changes of optical properties can be used as the "optical memory" effect. Tellurite glasses are known to be constituted by TeO_4 trigonal bipyramids which have one oxygen vacancy and a lone electron pair at one of the equatorial sites.[1-6] The ^{57}Fe-Mössbauer study of alkali tellurite[7,8] and alkaline-earth tellurite[8] glasses containing a small amount of iron revealed that the Fe^{3+} substitutes for Te^{4+}. It was also elucidated that change of skeleton structure takes place from the layer structure to a pseudo-chain or a three-dimensional network structure.[7,8] Mössbauer study of $xP_2O_5 \cdot (95-x)TeO_2 \cdot 5Fe_2O_3$ glasses showed a phase separation into tellurite-rich and phosphate-rich phases when the P_2O_5 content exceeds 25 mol%.[9] Isothermal annealing of $95TeO_2 \cdot 5Fe_2O_3$ glass caused crystallization followed by a decrease in the optical transmittance (T) in the IR region.[10] Change of the IR-transmittance was utilized for investigating the crystallization of glasses[10] when combined with the Johnson–Mehl–Avrami (JMA) equation[11] which was originally proposed for the crystallization in solution. Kissinger plot of DTA study was performed in order to estimate the E_a (activation energy) of crystallization in the bulk. X-Ray diffraction (XRD), IR absorption spectra, and ^{57}Fe-Mössbauer spectra have been utilized in order to characterize the crystalline phase precipitated in the glass matrix. Ar^+-laser irradiation was carried out in order to confirm the decrease of T due to the "optical memory" effect.

Experimental

Iron tellurite glass, $95TeO_2 \cdot 5Fe_2O_3$, was prepared by the conventional "crucible method"; weighed amount of TeO_2 and Fe_2O_3 of guaranteed reagent grade, placed in a platinum crucible after being pulverized, was fused at 850 °C for 1 h in an electric furnace. Iron tellurite glass of light brown color was prepared by immersing quickly the outer side of the crucible into ice-cold water. Isothermal annealing was performed similarly to the sample preparation; each sample was quenched with ice-cold water at the end of individual heat-treatment. The IR-transmission spectra were recorded on an FT-IR spectrometer (JASCO FT/IR-5000) with a small unpolished sample of thickness 0.50—0.90 mm. The IR absorption spectra were recorded on the same spectrometer by the KBr-disk method. The XRD pattern was recorded at a scanning rate of 1 degree min^{-1} with a Cu-$K\alpha$ source. Mössbauer measurements were performed by the constant acceleration method with the ^{57}Co-γ ray source (10 mCi, 3.7×10^8 Bq) diffused into a piece of palladium foil. A piece of iron foil enriched with iron-57 was used as a reference for the isomer shift (δ). Each Mössbauer spectrum was analyzed into one doublet peak by a least-squares method. DTA was conducted at a heating rate of 5—20 °C min^{-1} from room temperature to 700 °C with a reference of α-Al_2O_3. The Ar^+-laser irradiation with the wavelength of 514.5 and 483 nm was carried out at room temperature under the output power of 1.0 W.

Results and Discussion

Isothermal annealing of iron tellurite glass was carried out at different temperatures between T_g and $T_{c,max}$: maximal crystallization temperature in DTA. It can be confirmed with naked eye that the crystallization is initiated at the surface and spreads to the bulk. The XRD pattern shown in Fig. 1 indicates that the crystallized phase consists of paratellurite (α-TeO_2) and iron tellurite, of which diffraction peaks are marked with

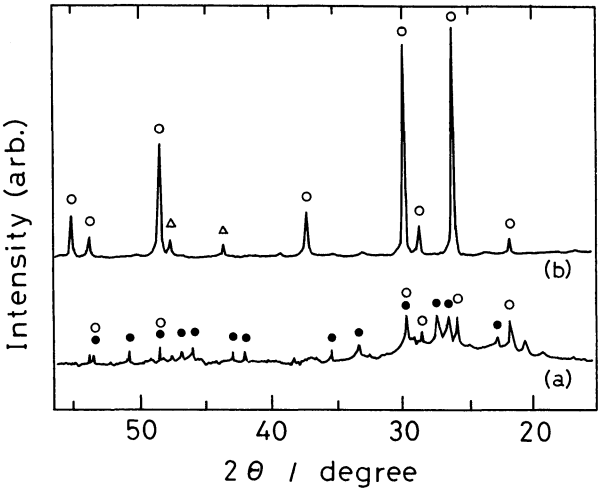

Fig. 1. XRD patterns of (a) $95TeO_2 \cdot 5Fe_2O_3$ glass annealed at 400 °C for 200 min and (b) reagent mixture of 95 mol% TeO_2 and 5 mol% Fe_2O_3. ○: paratellurite (α-TeO_2), ●: iron tellurite, △: Fe_2O_3.

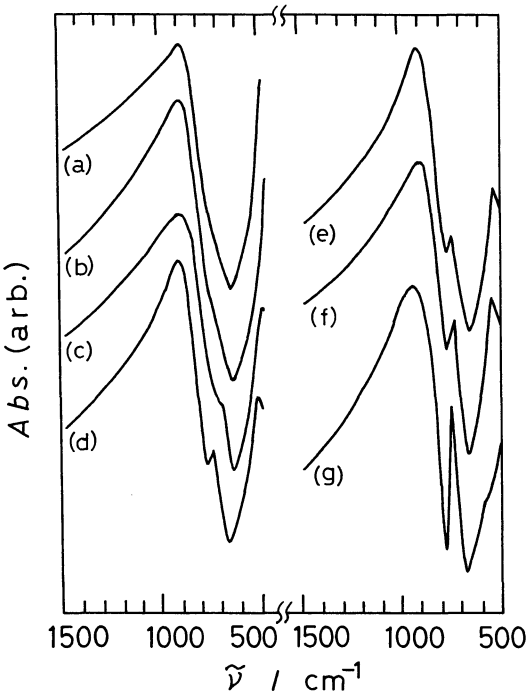

Fig. 2. IR absorption spectra of $95TeO_2 \cdot 5Fe_2O_3$ glass annealed at 400 °C for (a) 0 min, (b) 5 min, (c) 10 min, (d) 20 min, (e) 40 min, and (f) 200 min. (g): IR spectrum of reagent mixture of 95 mol% TeO_2 and 5 mol% Fe_2O_3.

open and closed circles, respectively. The XRD of the reagent mixture (95 mol% TeO_2 plus 5 mol% Fe_2O_3) is also shown for comparison, and the open circle and triangle indicate TeO_2 and Fe_2O_3, respectively.

The formation of α-TeO_2 is also observed in the IR absorption spectra. The peak appearing around 780 cm^{-1} in Figs. 2d—f is ascribed to the asymmetric Te–

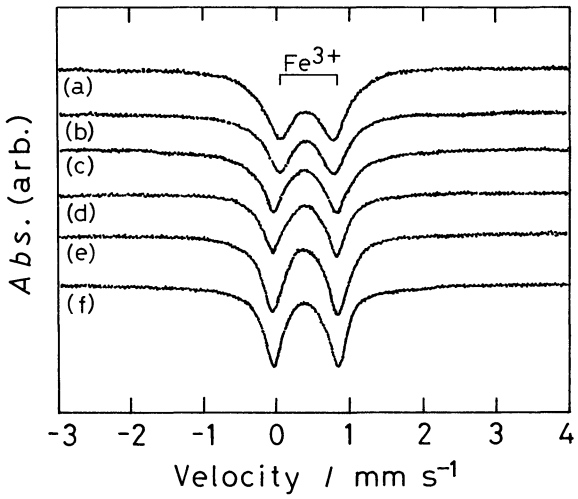

Fig. 3. Mössbauer spectra of $95TeO_2 \cdot 5Fe_2O_3$ glass annealed at 400 °C for (a) 0 min, (b) 5 min, (c) 10 min, (d) 20 min, (e) 40 min, and (f) 200 min.

O_{ax} stretching band of TeO_2. The IR spectrum of TeO_2 (reagent) is shown in Fig. 2g for comparison. The main peak due to the symmetric Te–O_{eq} band becomes sharp with the annealing, as is shown in Figs. 2a—f. (O_{ax} and O_{eq} indicate the oxygen atoms at axial and equatorial sites, respectively.) Formation of the iron tellurite is reflected in the change of ^{57}Fe-Mössbauer spectra shown in Fig. 3. Linewidth Γ (FWHM) of the broad doublet peak decreases from 0.57 mm s^{-1} (original glass, Fig. 3a) to 0.47 (Fig. 3b), 0.46 (Fig. 3c), and 0.44 mm s^{-1} (Figs. 3d—f) by the crystallization. This result indicates that the Fe^{3+} substituting for the Te^{4+} in the glass is precipitated in the crystalline iron tellurite. The δ (isomer shift) shows only a slight decrease from 0.39 mm s^{-1} to 0.38 (Figs. 3c and d) and 0.37 mm s^{-1} (Figs. 3e and f), indicating a decreased Fe^{3+}–O bond length and increased covalency. The Δ (quadrupole splitting) increases stepwise by the crystallization, e.g. 0.76→0.78→0.80→0.84→0.85→0.86 mm s^{-1}, as shown in Figs. 3a—f. This suggests that the crystalline phase of iron tellurite has a lower symmetry than the α-TeO_2 and original glass phase do; crystallization of $95TeO_2 \cdot 5Fe_2O_3$ glass is of disproportionate type from a homogeneous glass phase into the α-TeO_2 and iron tellurite phases with higher and lower symmetries, respectively. Such crystallization was also observed when a mayenite ($12CaO \cdot 7Al_2O_3$) phase with a lower symmetry precipitated in the calcium aluminate glass.[12]

Crystallization of the $95TeO_2 \cdot 5Fe_2O_3$ glass causes a drastic change of transmittance (T) in the IR-transmission spectra, as illustrated in Fig. 4. Similar result was obtained by the crystallization of calcium gallate glass, in which crystalline phases of $CaGa_2O_4$ and $CaFe_2O_4$ precipitated.[13,14] Decrease of T in the IR-transmission spectra is ascribed to the increased degree of scattering and reflection due to the crystalline phase. Figure 4 shows that the T decreases in the higher wave-number

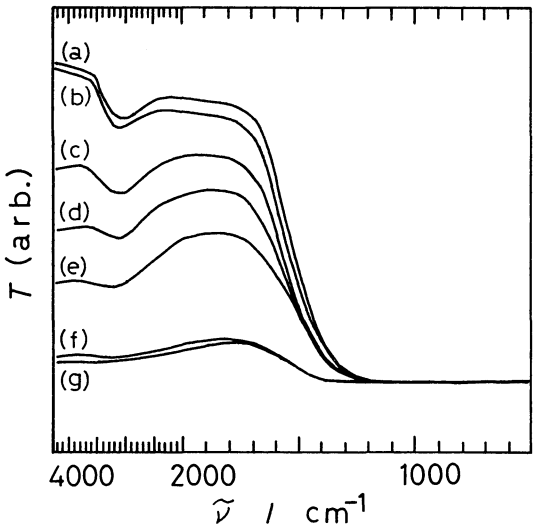

Fig. 4. IR-transmission spectra of $95TeO_2 \cdot 5Fe_2O_3$ glass annealed at 370°C for (a) 0 min, (b) 10 min, (c) 20 min, (d) 40 min, (e) 200 min, (f) 7000 min, and (g) 8000 min.

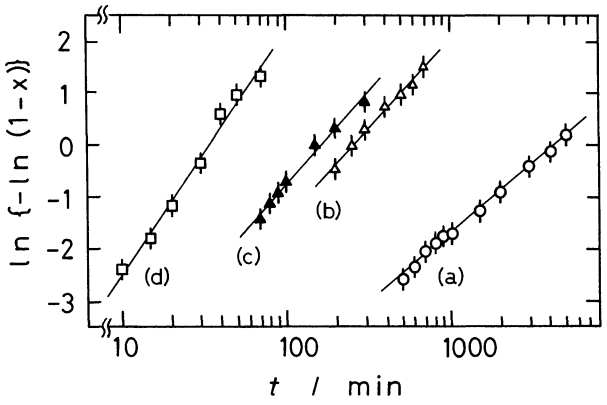

Fig. 5. JMA plot for the crystallization of $95TeO_2 \cdot 5Fe_2O_3$ glass annealed at (a) 370°C, (b) 380°C, (c) 390°C, and (d) 400°C.

region at first and then in the lower region, reflecting the growing size or thickness of the crystalline phase. Since the reduction rate of T is proportional to the degree of crystallization as observed with naked eye, the crystallization rate can be correlated to the decreased fraction of T, i.e. the crystallized fraction x can be approximated by

$$x = (T_0 - T_a)/(T_0 - T_b), \quad (1)$$

in which T_0 is the original T at the transmission edge (5.9 μm, 1690 cm^{-1}) at t=0. T_a is the transmittance (T) at t=a and T_b the minimal T obtained at the final stage of crystallization. The T_b was 1.0% when the $95TeO_2 \cdot 5Fe_2O_3$ glass was annealed at 370°C (Fig. 4), whereas it was 0% when annealed at 380 and 390°C. In the case of isothermal annealing, Johnson–Mehl–Avrami (JMA) equation[11] is useful for the kinetic study of crystallization. The JMA equation is expressed by

$$\ln\{-\ln(1-x)\} = n \ln t + \ln k, \quad (2)$$

in which n is the "Avrami index" indicating the mechanism of crystallization, i.e., the dimension of crystal growth and whether the crystallization is initiated at the surface or in the bulk. The JMA plot, $\ln\{-\ln(1-x)\}$ vs. $\ln t$, yields the slope n (Avrami index) of 1.0 (Fig. 5a) and 1.5 (Figs. 5b and c) which indicate that two- or three-dimensional crystallization takes place by the diffusion process.[11] The Avrami index of 2.0 obtained in the crystallization at 400°C (Fig. 5d) reflects a constant crystal growth in a two-dimensional manner.[11] The values of k obtained from the intercepts of the JMA plot (Fig. 5) are $(8.0\pm0.2)\times10^{-5}$, $(2.5\pm0.1)\times10^{-4}$, $(5.0\pm0.1)\times10^{-4}$, and $(7.4\pm0.1)\times10^{-4}$ when the glass sample was annealed at 370, 380, 390, and 400°C, respectively. The activation energy (E_a) of 2.9±0.3 eV obtained from the Arrhenius plot is identical to the Te^{4+}–O single bond energy obtained from the literature (3.0 eV[15]). This suggests that the cleavage of Te^{4+}–O bond triggers the crystallization initiating at the surface of the glass sample. This type of crystallization was also observed in aluminate and gallate glasses of which E_a's were identical to the Al–O and Ga–O single bond energies, respectively.[13,14]

It is interesting to compare the IR-transmission method with the conventional DTA method combined with the "Kissinger plot,"[16] by which E_a of crystallization in the bulk can be obtained by

$$\ln(T_{c,max}^2/\alpha) = -E_a/RT_{c,max} + \text{const.} \quad (3)$$

α is the heating rate and R the gas constant. The DTA curve of $95TeO_2 \cdot 5Fe_2O_3$ glass is shown in Fig. 6. The $T_{c,max}$ is the maximal exothermic temperature at which the crystallization becomes most frequent. They are observed at 423, 432, and 444°C when heated at 5, 10, and 20°C min^{-1}, respectively. The Kissinger plot is shown in Fig. 7, in which $\ln(T_{c,max}^2/\alpha)$ has a linear relationship with the $T_{c,max}^{-1}$. The slope of straight line shown in Fig. 7 yields the E_a of 2.3 eV, which is almost comparable to the E_a obtained from the IR-transmission method described above: 2.9±0.3 eV. These results suggest that the mechanism of crystallization in the bulk of $95TeO_2 \cdot 5Fe_2O_3$ glass is almost the same as that at the surface; crystallization in the bulk also proceeds in a two- or three-dimensional manner by the diffusion process.

The Kissinger plot has been used in the crystallization study of several binary tellurite glasses by Inoue and Nukui.[17] They elucidated that the E_a of several tellurite glasses falls in the range of 1.6—2.6 eV, although large E_a was obtained in the case of aluminum tellurite (3.7 eV) and magnesium tellurite (3.8 eV) glasses.[17] Formation

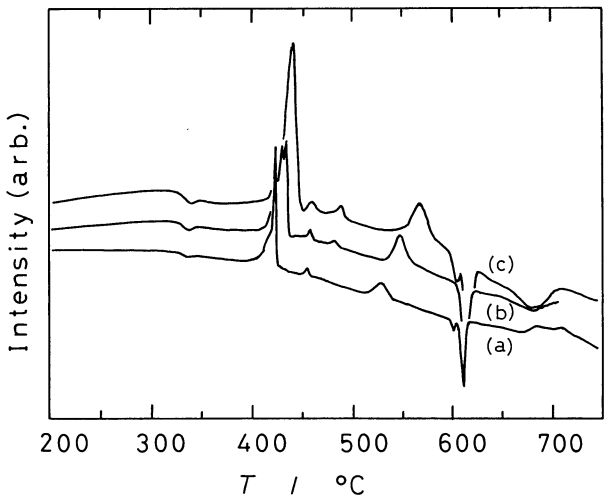

Fig. 6. DTA curves of $95TeO_2 \cdot 5Fe_2O_3$ glass recorded at heating rates (α) of (a) 5 °C min^{-1}, (b) 10 °C min^{-1}, and (c) 20 °C min^{-1}.

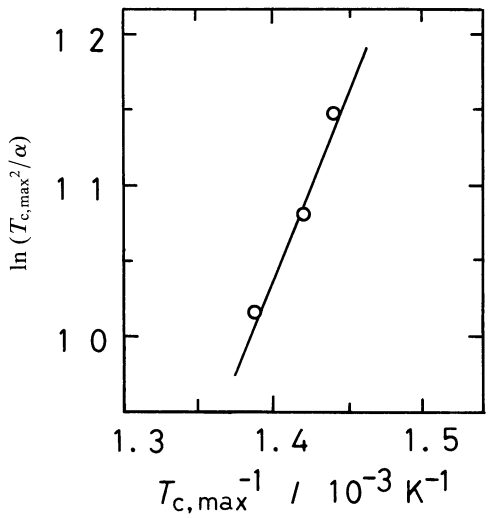

Fig. 7. Kissinger plot for the crystallization of $95TeO_2 \cdot 5Fe_2O_3$ glass.

of crystalline TeO_2 phase was confirmed by XRD in several tellurite glasses, and the E_a obtained for $90TeO_2 \cdot 10TiO_2$ glass (2.6 eV)[17] is comparable to that of $95TeO_2 \cdot 5Fe_2O_3$ glass (2.3 eV) obtained in this paper. The $90TeO_2 \cdot 10TiO_2$ glass has the $T_{c,max}$ (441 °C) which is comparable to that of the $95TeO_2 \cdot 5Fe_2O_3$ glass (423 °C) as illustrated in Figs. 6 and 7.

Ar^+-laser irradiation of 514.5 and 483 nm wavelength was carried out at room temperature. Figure 8 shows a distinct and gradual decrease of T caused by the irradiations of 1—40 s, similarly to the results of isothermal annealing performed at 370—400 °C (Fig. 4). The experimental result shown in Fig. 8 suggests that the crystallization takes place evidently by the laser irradiation at room temperature, and it is considered that the tellurite glass no doubt shows the "optical memory" effect.

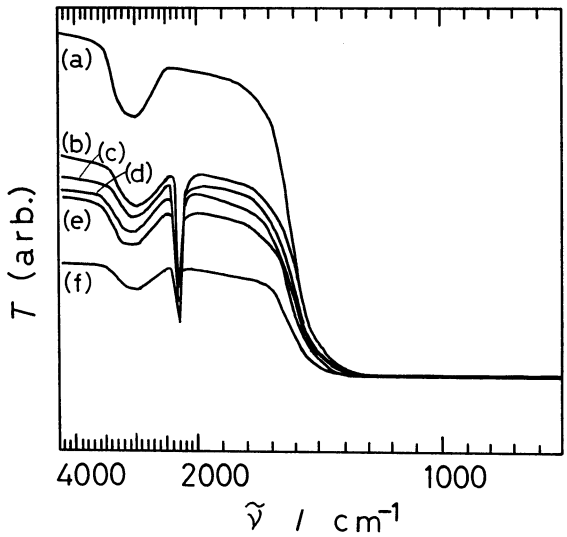

Fig. 8. IR-transmission spectra of $95TeO_2 \cdot 5Fe_2O_3$ glass after the Ar^+-laser irradiation (1.0 W) for (a) 0 s, (b) 1 s, (c) 2 s, (d) 10 s, (e) 20 s, and (f) 40 s.

Conclusions

1) IR-transmission spectroscopy is effective for investigating the crystallization of glass when combined with the Johnson–Mehl–Avrami (JMA) equation. Crystallization of $95TeO_2 \cdot 5Fe_2O_3$ glass proceeds in a two- or three-dimensional manner from the surface to the bulk.

2) Formation of paratellurite (α-TeO_2) and iron tellurite was confirmed by XRD, IR, and ^{57}Fe-Mössbauer measurements.

3) The E_a of 2.9±0.3 eV obtained by the IR-transmission method is identical to the Te^{4+}–O bond energy (3.0 eV) obtained from the literature. Cleavage of the Te^{4+}–O bond triggers the crystallization initiating at the surface.

4) The E_a obtained by the Kissinger plot of DTA method (2.3 eV) reflects the crystallization in the bulk, and it suggests that the mechanism of crystallization in the bulk is almost the same as that at the surface.

The authors are grateful to Professor Yasukuni Matsumoto, Fukuoka University, and Professor Toshirou Yagi, Hokkaido University, for useful discussion and help in the experiments. One of the authors (TN) is indebted to Tokuyama Science Foundation for financial support.

References

1) S. Neov, I. Gerassimova, K. Krezhov, B. Sydzhimov, and V. Kozhukharov, *Phys. Status Solidi A*, **47**, 743 (1978).

2) S. Neov, I. Gerassimova, V. Kozhukharov, and M. Marinov, *J. Mater. Sci.*, **15**, 1153 (1980).

3) P. A. V. Johnson, A. C. Wright, C. A. Yarker, and R. N. Sinclair, *J. Non-Cryst. Solids*, **81**, 163 (1986).

4) N. Mochida, K. Takahashi, K. Nakata, and S. Shibusawa, *Yogyo-Kyokai-Shi,* **86**, 317 (1978).
5) Y. Dimitriev, V. Dimitrov, and M. Arnaudov, *J. Mater. Sci.,* **14**, 723 (1979).
6) K. Tanaka, T. Yoko, H. Yamada, and K. Kamiya, *J. Non-Cryst. Solids,* **103**, 250 (1988).
7) T. Nishida, S. Saruwatari, and Y. Takashima, *Bull. Chem. Soc. Jpn.,* **61**, 4093 (1988).
8) T. Nishida, M. Yamada, H. Ide, and Y. Takashima, *J. Mater. Sci.,* **25**, 3546 (1990).
9) T. Nishida, M. Yamada, and Y. Takashima, *Bull. Chem. Soc. Jpn.,* in press (sheduled for publication in the September issue, 1992).
10) T. Nishida, M. Yamada, T. Ichii, Y. Matsumoto, T. Yagi, and Y. Takashima, Proc. Int. Conf. Sci. Tech. New Glasses, The Ceramic Society of Japan, Tokyo (1991), pp. 83—88.
11) M. Avrami, *J. Chem. Phys.,* **8**, 212 (1940).
12) T. Nishida, H. Ide, T. Shinmyozu, Y. Takashima, and Y. Matsumoto, *Jpn. J. Appl. Phys.,* **29**, 1293 (1990).
13) T. Nishida, M. Yamada, T. Ichii, Y. Matsumoto, T. Yagi, and Y. Takashima, Proc. VII Int. Conf. Phys. Non-Cryst. Solids, Cambridge (1991), Taylor & Francis, London (1992), pp. 392—396.
14) T. Nishida, T. Ichii, and Y. Takashima, *J. Mater. Chem.,* **2**, in press (scheduled for publication in the July issue, 1992).
15) D. Chakravorty, "Modern Aspects of Solid State Chemistry," Plenum Press, New York (1970), p. 398.
16) H. E. Kissinger, *Anal. Chem.,* **29**, 1702 (1957).
17) S. Inoue and A. Nukui, Proc. Int. Conf. Sci. Tech. New Glasses, The Ceramic Society of Japan, Tokyo (1991), pp. 77—82.